

1 **LSLQ: AN ITERATIVE METHOD FOR LINEAR LEAST-SQUARES**
 2 **WITH AN ERROR MINIMIZATION PROPERTY***

3 RON ESTRIN[†], DOMINIQUE ORBAN[‡], AND MICHAEL A. SAUNDERS[§]

4 **Abstract.** We propose an iterative method named LSLQ for solving linear least-squares problems
 5 of any shape. The method is based on the [Golub and Kahan \(1965\)](#) process, where the dominant cost
 6 is products with the linear operator and its transpose. In the rank-deficient case, LSLQ identifies
 7 the minimum-length least-squares solution. LSLQ is formally equivalent to SYMMLQ applied to the
 8 normal equations, so that the current estimate’s Euclidean norm increases monotonically while the
 9 associated error norm decreases monotonically. We provide lower and upper bounds on the error in
 10 the Euclidean norm along the LSLQ iterations. The upper bound translates to an upper bound on the
 11 error norm along the LSQR iterations, which was previously unavailable, and provides an error-based
 12 stopping criterion involving a transition to the LSQR point. We report numerical experiments on
 13 standard test problems and on a full-wave inversion problem arising from geophysics in which an
 14 approximate least-squares solution corresponds to an approximate gradient of a relevant penalty
 15 function that is to be minimized.

16 **1. Introduction.** We propose an iterative method (LSLQ) for solving two ubiqui-
 17 tous problems in computational science—the least-squares problem and the least-norm
 18 problem:

19 (LS)
$$\underset{x \in \mathbb{R}^n}{\text{minimize}} \quad \frac{1}{2} \|Ax - b\|^2,$$

20 (LN)
$$\underset{x \in \mathbb{R}^n}{\text{minimize}} \quad \frac{1}{2} \|x\|^2 \quad \text{subject to } Ax = b,$$

21

22 both of which include consistent linear systems $Ax = b$ as a special case. The norm
 23 $\|\cdot\|$ is Euclidean and A may be an m -by- n matrix, but we assume more generally that
 24 $A : \mathbb{R}^n \rightarrow \mathbb{R}^m$ is a linear operator because only operator-vector products of the form
 25 Au and $A^T v$ are required. We often refer to the optimality conditions of (LS), namely
 26 the normal equations

27 (NE)
$$A^T Ax = A^T b.$$

28 When $Ax = b$ is consistent, LSLQ identifies a solution of (LN). If $\text{rank}(A) < n$, LSLQ
 29 finds the minimum-length solution (MLS) $x_* = A^\dagger b$, where A^\dagger is the pseudoinverse.

30 **Motivation: monitoring the error.** We briefly describe why an iterative
 31 method for least squares with an error minimization property is of interest.

32 [Van Leeuwen and Herrmann \(2013\)](#) describe a penalty method for PDE-constrained
 33 optimization in the context of a seismic inverse problem. The penalty objective
 34 $\phi_\rho(\mathbf{m}, \mathbf{u})$ depends on the control variable \mathbf{m} and the wavefields \mathbf{u} , where $\rho > 0$ is
 35 a penalty parameter. For fixed values of ρ and \mathbf{m} , the wavefields $\mathbf{u}(\mathbf{m})$ satisfying

*Version of January 11, 2018.

[†]Institute for Computational and Mathematical Engineering, Stanford University, Stanford, CA, USA. E-mail: restrin@stanford.edu.

[‡]GERAD and Department of Mathematics and Industrial Engineering, École Polytechnique, Montréal, QC, Canada. E-mail: dominique.orban@gerad.ca. Research partially supported by an NSERC Discovery Grant.

[§]Systems Optimization Laboratory, Department of Management Science and Engineering, Stanford University, Stanford, CA, USA. E-mail: saunders@stanford.edu. Research partially supported by the National Institute of General Medical Sciences of the National Institutes of Health, award U01GM102098.

36 $\nabla_{\mathbf{u}}\phi_{\rho}(\mathbf{m}, \mathbf{u}(\mathbf{m})) = 0$ can be found as the solution of a linear least-squares (LS) problem
 37 in \mathbf{u} . The gradient of ϕ with respect to \mathbf{m} is subsequently expressed as a linear function
 38 of $\mathbf{u}(\mathbf{m})$, say

$$39 \quad \nabla_{\mathbf{m}}\phi_{\rho}(\mathbf{m}, \mathbf{u}(\mathbf{m})) = G \mathbf{u}(\mathbf{m}) - g$$

40 for a certain matrix G and vector g . Assume now that an inexact solution $\tilde{\mathbf{u}}$ of the LS
 41 problem for $\mathbf{u}(\mathbf{m})$ is determined. The error in \mathbf{u} translates directly into an error in
 42 the gradient of the penalty function, for

$$43 \quad (1) \quad \|\nabla_{\mathbf{m}}\phi_{\rho}(\mathbf{m}, \mathbf{u}) - \nabla_{\mathbf{m}}\phi_{\rho}(\mathbf{m}, \tilde{\mathbf{u}})\| \leq \|G\| \|\mathbf{u} - \tilde{\mathbf{u}}\|, \quad \mathbf{u} \equiv \mathbf{u}(\mathbf{m}).$$

44 If a derivative-based optimization method is to be used to minimize the penalty
 45 function, there is interest in a method to approximate \mathbf{u} in which the error is monoton-
 46 ically decreasing. Indeed, the convergence properties of derivative-based optimization
 47 methods are not altered provided the gradient is computed sufficiently accurately in
 48 the sense that the left-hand side of (1) is sufficiently small compared to $\|\nabla_{\mathbf{m}}\phi_{\rho}(\mathbf{m}, \mathbf{u})\|$
 49 (Conn, Gould, and Toint, 2000, §8.4.1.1).

50 In the following sections, we introduce the LSLQ method. We now comment on
 51 the necessity for LSLQ in order to monitor the error reliably. At this stage, it is
 52 sufficient to say that LSLQ applied to problem (LS) is equivalent to SYMMLQ (Paige
 53 and Saunders, 1975) applied to (NE). LSLQ fits in the category of Krylov-subspace
 54 methods based on the Golub and Kahan (1965) process, and in that sense is related to
 55 LSQR (Paige and Saunders, 1982a) and LSMR (Fong and Saunders, 2011) (equivalent
 56 to CG and MINRES applied to (NE)). As far as error monitoring is concerned, the
 57 key advantage that LSLQ inherits from SYMMLQ is that the solution estimate is
 58 updated along orthogonal directions. As a consequence, the solution norm increases
 59 and the error decreases along the iterations. It happens that both LSQR and LSMR
 60 share those properties (Fong and Saunders, 2012, Table 5.2) but with important
 61 differences. First, LSLQ's orthogonal updates suggest error lower and upper bounds
 62 initially developed for SYMMLQ by Estrin, Orban, and Saunders (2016), and which
 63 are the subject of section 4. Second, the error is *minimized* in LSLQ, while it is only
 64 monotonic in LSQR and LSMR. In spite of the latter observation, the error along
 65 the LSQR and LSMR iterations is typically smaller than for the LSLQ iterations by
 66 a few orders of magnitude—see Proposition 1. This is not a contradiction because
 67 LSLQ minimizes the error in a transformation of the Krylov subspace. Figure 1
 68 illustrates a typical scenario, where the error is represented along the LSQR, LSMR,
 69 and LSLQ iterations on two over-determined problems arising from an animal breeding
 70 application (Hegland, 1990, 1993), and where we consider that the solution obtained
 71 with a complete orthogonal decomposition is the exact solution.

72 It appears from Figure 1 that LSQR is more appealing than LSLQ if one is
 73 interested in minimizing the error. The difficulty is that LSQR does not lend itself
 74 to obvious error lower and upper bounds because it is not naturally formulated in
 75 terms of the Euclidean norm and its solution estimate is not updated along orthogonal
 76 directions. Estimates of the error in the conjugate gradient (CG) method (Hestenes
 77 and Stiefel, 1952) applied to a symmetric and positive definite system have been
 78 developed in the literature, an effort led chiefly by Meurant (2005). Those estimates
 79 could be applied to LSQR but unfortunately they are only estimates and have not
 80 been proved to be lower or upper bounds. Thus it is difficult to terminate the LSQR
 81 iterations reliably with a guaranteed error level. Fortunately, SYMMLQ is closely
 82 related to CG and it is possible to transition cheaply from a SYMMLQ iterate to a
 83 corresponding CG iterate. LSLQ inherits that property and it is possible to transition

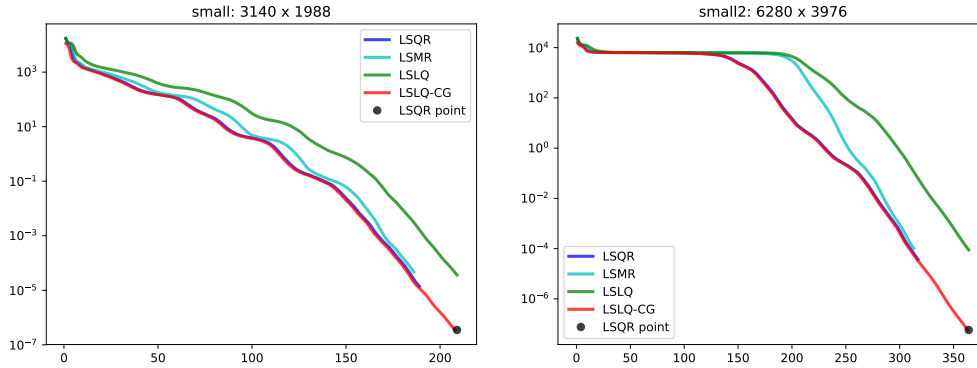


FIG. 1. Error along the LSQR, LSMR and LSLQ iterations on problems *small* and *small2* from the animal breeding set. The red curve corresponds to the LSQR iterates generated as a by-product during the LSLQ iterations. The horizontal axis represents the number of iterations (each involving a product with A and a product with A^T).

84 to a related LSQR iterate at any iteration. The red curve in Figure 1 represents the
 85 error observed at each LSQR point obtained by transitioning from the then-current
 86 LSLQ point. Note the high accuracy to which the red and blue curves match; they are
 87 essentially superposed. The black dot represents the error observed after transitioning
 88 from the final LSLQ iterate to the LSQR point. Note also that because the stopping
 89 rule for all methods involves the residual of the normal equations, the curves end at
 90 different abscissae.

91 Our main objective is to exploit the reliable lower and upper bounds on the LSLQ
 92 error based on those developed for SYMMLQ by Estrin et al. (2016). The upper
 93 bound on the LSLQ errors combined with the tight relationship between LSLQ and
 94 LSQR leads to an upper bound on the LSQR error. Thus it becomes possible to end
 95 the LSLQ iterations as soon as it becomes apparent that the upper bound on the
 96 LSQR error is below a prescribed tolerance.

97 Both problems used in Figure 1 are rank-deficient and the curves indicate that
 98 all methods tested identify the MLS solution. Problem *small2* is included in the
 99 illustration because it is an example where the error plateaus. We return to this point
 100 in section 4.

101 We do not consider LSMR further here for two reasons. First, it is a consequence of
 102 (Hestenes and Stiefel, 1952, Theorem 7:5) that the LSMR error is monotonic but equal
 103 to or larger than that of LSQR—see also (Fong and Saunders, 2012, Theorem 2.4).
 104 Second, LSMR is a variant of MINRES (Paige and Saunders, 1975) and we know of
 105 no result relating the errors along the MINRES iterations on a symmetric positive
 106 definite system to those along the SYMMLQ iterations.

107 **Notation.** We use Householder notation (A , b , β for matrix, vector, scalar) with
 108 the exception of c and s , which denote scalars used to define reflections. Unless specified
 109 otherwise, $\|A\|$ and $\|x\|$ denote the Euclidean norm of matrix A and vector x . For
 110 rectangular A , we order its singular values according to $\sigma_1 \geq \sigma_2 \geq \dots \geq \sigma_{\min(m,n)} \geq 0$.
 111 For symmetric positive definite M , we define the M -norm of u via $\|u\|_M^2 := u^T M u$.

112 **2. Derivation of the method.** In this section, we describe LSLQ using the
 113 process/method/implementation framework.

114 **2.1. The Golub-Kahan process.** LSLQ is based on the [Golub and Kahan](#)
 115 [\(1965\)](#) process described as [Algorithm 1](#), with A and b as in [\(LS\)](#) or [\(LN\)](#). In line 1,
 116 $\beta_1 u_1 = b$ is short for “ $\beta_1 = \|b\|$; if $\beta_1 = 0$ then exit; else $u_1 = b/\beta_1$ ”. Similarly for
 117 line 2 and the main loop. In exact arithmetic, the algorithm will terminate with
 118 $k = \ell \leq \min(m, n)$ and either $\alpha_{\ell+1}$ or $\beta_{\ell+1} = 0$.

Algorithm 1 Golub-Kahan Bidiagonalization Process

Require: A, b

- 1: $\beta_1 u_1 = b$
 - 2: $\alpha_1 v_1 = A^T u_1$
 - 3: **for** $k = 1, 2, \dots$ **do**
 - 4: $\beta_{k+1} u_{k+1} = A v_k - \alpha_k u_k$
 - 5: $\alpha_{k+1} v_{k+1} = A^T u_{k+1} - \beta_{k+1} v_k$
 - 6: **end for**
-

119 We define $U_k := [u_1 \ \dots \ u_k]$, $V_k := [v_1 \ \dots \ v_k]$, and

$$120 \quad (2) \quad L_k := \begin{bmatrix} \alpha_1 & & & & & \\ & \beta_2 & & & & \\ & & \alpha_2 & & & \\ & & & \ddots & & \\ & & & & \beta_k & \\ & & & & & \alpha_k \end{bmatrix}, \quad B_k := \begin{bmatrix} \alpha_1 & & & & & \\ \beta_2 & \alpha_2 & & & & \\ & & \ddots & & & \\ & & & \ddots & & \\ & & & & \beta_k & \alpha_k \\ & & & & & \beta_{k+1} \end{bmatrix} = \begin{bmatrix} L_k \\ \beta_{k+1} e_k^T \end{bmatrix}.$$

121 The situation after k iterations of [Algorithm 1](#) can be summarized as

$$122 \quad (3a) \quad AV_k = U_{k+1} B_k,$$

$$123 \quad (3b) \quad A^T U_{k+1} = V_k B_k^T + \alpha_{k+1} v_{k+1} e_{k+1}^T = V_{k+1} L_{k+1}^T,$$

125 and the identities $U_k^T U_k = I_k$ and $V_k^T V_k = I_k$ are satisfied in exact arithmetic.

126 **2.2. LSLQ: method.** By definition, LSLQ applied to [\(LS\)](#) is equivalent to
 127 SYMMLQ applied to [\(NE\)](#). The identities [\(3\)](#) yield

$$128 \quad \begin{aligned} A^T A V_k &= A^T U_{k+1} B_k \\ &= V_k B_k^T B_k + \alpha_{k+1} v_{k+1} e_{k+1}^T B_k \\ &= V_k B_k^T B_k + \alpha_{k+1} \beta_{k+1} v_{k+1} e_k^T \\ 130 \quad (4) \quad &= V_{k+1} H_k, \end{aligned}$$

133 where

$$134 \quad (5) \quad H_k := \begin{bmatrix} B_k^T B_k \\ \alpha_{k+1} \beta_{k+1} e_k^T \end{bmatrix},$$

135 while lines 1 and 2 of [Algorithm 1](#) yield $A^T b = \alpha_1 \beta_1 v_1$. From here on, we use the
 136 shorthand

$$137 \quad (6) \quad \bar{\alpha}_k := \alpha_k^2 + \beta_{k+1}^2, \quad \text{and} \quad \bar{\beta}_k := \alpha_k \beta_k, \quad k = 1, 2, \dots$$

138 As noted by [Fong and Saunders \(2011\)](#), the above characterizes the situation after
 139 $k + 1$ steps of the [Lanczos \(1950\)](#) process applied to $A^T A$ with initial vector $A^T b$. For

140 all $k \geq 1$, we denote

$$141 \quad (7) \quad T_k := B_k^T B_k = \begin{bmatrix} \bar{\alpha}_1 & \bar{\beta}_2 & & \\ \bar{\beta}_2 & \bar{\alpha}_2 & \ddots & \\ & \ddots & \ddots & \bar{\beta}_k \\ & & \bar{\beta}_k & \bar{\alpha}_k \end{bmatrix}, \quad H_k = \begin{bmatrix} T_k \\ \bar{\beta}_{k+1} e_k^T \end{bmatrix}.$$

142 Note that T_k is k -by- k and tridiagonal, and H_k is $(k+1)$ -by- k .

143 The k -th iteration of CG applied to (NE) computes $x_k^C = V_k y_k^C$, where y_k^C is the
144 solution of the subproblem

$$145 \quad (8) \quad T_k y_k^C = \bar{\beta}_1 e_1.$$

146 The resulting x_k^C can be shown to solve the subproblem

$$147 \quad (9) \quad \underset{x \in \mathcal{K}_k}{\text{minimize}} \quad \|x_\star - x\|_{A^T A},$$

148 where $\mathcal{K}_k := \text{Span}\{A^T b, (A^T A)A^T b, \dots, (A^T A)^k A^T b\}$ is the k -th Krylov subspace
149 associated with $A^T A$ and $A^T b$. LSQR (Paige and Saunders, 1982a,b) is equivalent
150 in exact arithmetic. By contrast, the k -th iteration of SYMMLQ applied to (NE)
151 computes y_k^L as the solution of

$$152 \quad (10) \quad \underset{y}{\text{minimize}} \quad \frac{1}{2} \|y\|^2 \quad \text{subject to} \quad H_{k-1}^T y = \bar{\beta}_1 e_1,$$

153 and sets $x_k^L := V_k y_k^L$. Note that H_{k-1}^T is the first $k-1$ rows of T_k and may be written
154 as $H_{k-1}^T = B_{k-1}^T L_k$. It can be shown that x_k^L solves the subproblem

$$155 \quad (11) \quad \underset{x \in A^T A \mathcal{K}_{k-1}}{\text{minimize}} \quad \|x_\star - x\|.$$

156 One important distinction between (9) and (11) is that $x_k^C \in \mathcal{K}_k$ while $x_k^L \in (A^T A)\mathcal{K}_{k-1}$,
157 a subset of \mathcal{K}_k . By construction, $\|x_\star - x_k\|$ is monotonic along the LSLQ iterates,
158 but as mentioned earlier, it also happens to be monotonic along the LSQR iterates.
159 Somewhat surprisingly, the error is always smaller along the LSQR iterates than along
160 the LSLQ iterates, as formalized by the next result.

161 **PROPOSITION 1.** *Let $x_k^C = V_k y_k^C$ and $x_k^L = V_k y_k^L$ with y_k^C and y_k^L defined as in
162 (8) and (10). Then, for all k ,*

$$163 \quad \|x_k^L\| \leq \|x_k^C\|,$$

$$164 \quad \|x_\star - x_k^C\| \leq \|x_\star - x_k^L\|.$$

166 *Proof.* The result follows from applying (Estrin et al., 2016, Theorem 6) to (NE). \square

167 Note first that Proposition 1 holds whether A has full column rank or not. Note
168 also that Proposition 1 does not contradict the definition of LSLQ as minimizing the
169 error because the latter is not minimized over the same subspace as that used during
170 the k -th iteration of LSQR.

171 In the next section we describe the implementation of LSLQ, and we return to
172 the two errors in section 4.

173 **2.3. LSLQ: implementation.** We identify y_k^L by way of an LQ factorization of
 174 H_{k-1}^T , which we compute via an implicit LQ factorization of $T_k = B_k^T B_k$. As in LSQR
 175 and LSMR we begin with the QR factorization

$$176 \quad (12) \quad P_k^T [B_k \quad \beta_1 e_1] = \begin{bmatrix} R_k & g_k \\ 0 & \psi'_{k+1} \end{bmatrix}, \quad R_k := \begin{bmatrix} \gamma_1 & \delta_2 & & \\ & \gamma_2 & \ddots & \\ & & \ddots & \delta_k \\ & & & \gamma_k \end{bmatrix}, \quad g_k = \begin{bmatrix} \psi_1 \\ \vdots \\ \psi_k \end{bmatrix},$$

177 where $P_k^T = P_{k,k+1} \dots P_{2,3} P_{1,2}$ is a product of orthogonal reflections. The j -th
 178 reflection $P_{j,j+1}$ is designed to zero out the sub-diagonal element β_{j+1} in B_k . With
 179 $\bar{\gamma}_1 := \alpha_1$ it may be represented as

$$180 \quad (13) \quad \begin{matrix} & j & j+1 & & j & j+1 & & j & j+1 \\ j & \begin{bmatrix} c'_j & s'_j \\ s'_j & -c'_j \end{bmatrix} & \begin{bmatrix} \bar{\gamma}_j & \\ & \alpha_{j+1} \end{bmatrix} & = & \begin{bmatrix} \gamma_j & \delta_{j+1} \\ & \bar{\gamma}_{j+1} \end{bmatrix}, \\ j+1 & & & & & & & & \end{matrix}$$

181 where $\gamma_j = (\bar{\gamma}_j^2 + \beta_{j+1}^2)^{\frac{1}{2}}$, $c'_j = \bar{\gamma}_j/\gamma_j$, $s'_j = \beta_{j+1}/\gamma_j$, and

$$182 \quad (14) \quad \begin{aligned} \delta_{j+1} &= s'_j \alpha_{j+1}, \\ \bar{\gamma}_{j+1} &= -c'_j \alpha_{j+1}. \end{aligned}$$

183 The rotations apply to the right-hand side $\beta_1 e_1$ to produce g_k defined by the recurrence

$$184 \quad (15) \quad \psi'_1 = \beta_1, \quad \psi_k = c'_k \psi'_k, \quad \psi'_{k+1} = s'_k \psi'_k, \quad k = 1, 2, \dots$$

185 It will be convenient to use the notation $g'_{k+1} = [g_k^T \quad \psi'_{k+1}]^T$.

186 The QR factors of B_k give the Cholesky factorization $T_k = R_k^T R_k$. To form LQ
 187 factors of T_k we take the LQ factorization

$$188 \quad (16) \quad R_k = \bar{M}_k Q_k, \quad \bar{M}_k := \begin{bmatrix} \varepsilon_1 & & & \\ \eta_2 & \varepsilon_2 & & \\ & \ddots & \ddots & \\ & & \eta_k & \bar{\varepsilon}_k \end{bmatrix}.$$

189 Initially, $\bar{\varepsilon}_1 = \gamma_1$ so that $R_1 = \bar{M}_1$. We use the notation of [Paige and Saunders \(1975\)](#)
 190 to indicate that \bar{M}_k differs from the leading k -by- k submatrix M_k of \bar{M}_{k+1} in the
 191 (k, k) -th element only, which is updated to ε_k once $\delta_{k+1} = \alpha_{k+1} \beta_{k+1} / \gamma_k$ is computed.
 192 This results in the plane reflection $Q_{k,k+1}$ defined by

$$193 \quad (17) \quad \begin{matrix} & k & k+1 & & k & k+1 & & k & k+1 \\ k & \begin{bmatrix} \bar{\varepsilon}_k & \delta_{k+1} \\ & \gamma_{k+1} \end{bmatrix} & \begin{bmatrix} c_k & s_k \\ s_k & -c_k \end{bmatrix} & = & \begin{bmatrix} \varepsilon_k & \\ & \bar{\varepsilon}_{k+1} \end{bmatrix}, \\ k+1 & & & & & & & & \end{matrix}$$

194 where $\varepsilon_k = (\bar{\varepsilon}_k^2 + \delta_{k+1}^2)^{\frac{1}{2}}$, $c_k = \bar{\varepsilon}_k/\varepsilon_k$, $s_k = \delta_{k+1}/\varepsilon_k$, and

$$195 \quad (18) \quad \begin{aligned} \eta_{k+1} &= \gamma_{k+1} s_k, \\ \bar{\varepsilon}_{k+1} &= -\gamma_{k+1} c_k. \end{aligned}$$

196 Combining (12) and (16) gives

$$197 \quad H_{k-1}^T = B_{k-1}^T L_k = [B_{k-1}^T B_{k-1} \quad \alpha_k \beta_k e_{k-1}] = R_{k-1}^T [R_{k-1} \quad \delta_k e_{k-1}].$$

198 By construction,

$$199 \quad R_k = \begin{bmatrix} R_{k-1} & \delta_k e_{k-1} \\ & \gamma_k \end{bmatrix} = \bar{M}_k Q_k = \begin{bmatrix} M_{k-1} & 0 \\ \eta_k e_{k-1}^T & \bar{\varepsilon}_k \end{bmatrix} Q_k$$

200 and we obtain the LQ factorization

$$201 \quad H_{k-1}^T = R_{k-1}^T [M_{k-1} \quad 0] Q_k = [R_{k-1}^T M_{k-1} \quad 0] Q_k.$$

202 With the solution of $H_{k-1}^T y_k^L = \bar{\beta}_1 e_1$ in mind, we consider the system $R_k^T t_k = \alpha_1 \beta_1 e_1$

203 and obtain $t_k := [\tau_1 \quad \dots \quad \tau_k]^T$ by the recursion

$$204 \quad (19) \quad \begin{aligned} \tau_1 &:= \alpha_1 \beta_1 / \gamma_1, \\ \tau_j &:= -\tau_{j-1} \delta_j / \gamma_j, \quad j = 2, \dots, k. \end{aligned}$$

205 We also consider the systems $M_{k-1} z_{k-1} = t_{k-1}$ and $\bar{M}_k \bar{z}_k := t_k$ and obtain $z_{k-1} :=$

206 $[\zeta_1 \quad \dots \quad \zeta_{k-1}]^T$ and $\bar{z}_k = [z_{k-1}^T \quad \bar{\zeta}_k]^T$ by the recursion

$$207 \quad (20) \quad \begin{aligned} \zeta_1 &= \tau_1 / \varepsilon_1, \\ \zeta_j &= (\tau_j - \zeta_{j-1} \eta_j) / \varepsilon_j, \quad j = 2, \dots, k-1, \\ \bar{\zeta}_k &= (\tau_k - \zeta_{k-1} \eta_k) / \bar{\varepsilon}_k = \zeta_k / c_k. \end{aligned}$$

208 Then $y_k^L = Q_k^T \begin{bmatrix} z_{k-1} \\ 0 \end{bmatrix}$ solves (10), while $y_k^C = Q_k^T \bar{z}_k$ solves (8).

209 Now let $\bar{W}_k := V_k Q_k^T = [w_1 \quad \dots \quad w_{k-1} \quad \bar{w}_k] = [W_{k-1} \quad \bar{w}_k]$. Starting with

210 $x_1^L := 0$ and $x_1^C := 0$ we obtain

$$211 \quad (21) \quad x_k^L = V_k y_k^L = V_k Q_k^T \begin{bmatrix} z_{k-1} \\ 0 \end{bmatrix} = \bar{W}_k \begin{bmatrix} z_{k-1} \\ 0 \end{bmatrix} = W_{k-1} z_{k-1} = x_{k-1}^L + \zeta_{k-1} w_{k-1},$$

$$212 \quad (22) \quad x_k^C = V_k Q_k^T \bar{z}_k = \bar{W}_k \bar{z}_k = W_{k-1} z_{k-1} + \bar{\zeta}_k \bar{w}_k = x_k^L + \bar{\zeta}_k \bar{w}_k.$$

214 Thus, as in SYMMLQ it is always possible to transfer to the CG point. In terms of

215 error, Proposition 1 indicates that transferring is always desirable.

216 At the next iteration we have $\bar{W}_{k+1} = V_{k+1} Q_{k+1}^T$, where

$$217 \quad \begin{bmatrix} \bar{w}_k & v_{k+1} \end{bmatrix} \begin{bmatrix} c_k & s_k \\ s_k & -c_k \end{bmatrix} = \begin{bmatrix} w_k & \bar{w}_{k+1} \end{bmatrix}.$$

218 With $\bar{w}_1 := v_1$ this gives

$$219 \quad (23a) \quad w_k = c_k \bar{w}_k + s_k v_{k+1},$$

$$220 \quad (23b) \quad \bar{w}_{k+1} = s_k \bar{w}_k - c_k v_{k+1}.$$

222 Because the columns of W_{k-1} and \bar{W}_k are orthonormal in exact arithmetic, we have

$$223 \quad (24) \quad \|x_k^L\|^2 = \|W_{k-1} z_{k-1}\|^2 = \|z_{k-1}\|^2 = \sum_{j=1}^{k-1} \zeta_j^2 = \|x_{k-1}^L\|^2 + \zeta_{k-1}^2,$$

$$224 \quad (25) \quad \|x_k^C\|^2 = \|x_k^L\|^2 + \bar{\zeta}_k^2.$$

226 **2.4. Residual estimates.** The k -th LSLQ residual is defined as $r_k^L := b - Ax_k^L$.
 227 We use the definition of $x_k^L = V_k y_k^L$, (3), (12) and (16) to express it as

$$\begin{aligned}
 r_k^L &= b - AV_k y_k^L = U_{k+1} \left(\beta_1 e_1 - B_k y_k^L \right) \\
 &= U_{k+1} P_k \left(\beta_1 P_k^T e_1 - \begin{bmatrix} R_k \\ 0 \end{bmatrix} y_k^L \right) \\
 &= U_{k+1} P_k \left(g'_{k+1} - \begin{bmatrix} \overline{M}_k Q_k \\ 0 \end{bmatrix} y_k^L \right) \\
 &= U_{k+1} P_k \left(g'_{k+1} - \begin{bmatrix} \overline{M}_k \\ 0 \end{bmatrix} \begin{bmatrix} z_{k-1} \\ 0 \end{bmatrix} \right) \\
 &= U_{k+1} P_k \left(g'_{k+1} - \begin{bmatrix} M_{k-1} z_{k-1} \\ \eta_k \zeta_{k-1} \\ 0 \end{bmatrix} \right) \\
 &= U_{k+1} P_k \left(\begin{bmatrix} g_{k-1} \\ \psi_k \\ \psi'_{k+1} \end{bmatrix} - \begin{bmatrix} t_{k-1} \\ \eta_k \zeta_{k-1} \\ 0 \end{bmatrix} \right),
 \end{aligned}$$

229 where g'_{k+1} is defined in (12) and (15). It is not immediately obvious that $g_{k-1} = t_{k-1}$,
 230 but note that (12) yields $\begin{bmatrix} R_{k-1}^T & 0 \end{bmatrix} P_{k-1}^T = B_{k-1}^T$, so that

$$231 \quad R_{k-1}^T g_{k-1} = \begin{bmatrix} R_{k-1}^T & 0 \end{bmatrix} \begin{bmatrix} g_{k-1} \\ \psi'_k \end{bmatrix} = B_{k-1}^T \beta_1 e_1 = \alpha_1 \beta_1 e_1 = R_{k-1}^T t_{k-1}$$

232 as long as $\gamma_{k-1} \neq 0$. Therefore, if the process does not terminate, we have $g_{k-1} = t_{k-1}$
 233 as announced. By orthogonality of U_{k+1} and P_k we have

$$234 \quad (26) \quad \|r_k^L\|^2 = \left\| \begin{bmatrix} 0 \\ \psi_k - \eta_k \zeta_{k-1} \\ \psi'_{k+1} \end{bmatrix} \right\|^2 = (\psi_k - \eta_k \zeta_{k-1})^2 + (\psi'_{k+1})^2.$$

235 The residual norm for the CG-point can also be computed as

$$236 \quad r_k^C := b - Ax_k^C = U_{k+1} P_k \left(P_k^T \beta_1 e_1 - \begin{bmatrix} R_k \\ 0 \end{bmatrix} y_k^C \right) = U_{k+1} P_k \left(\begin{bmatrix} g_k \\ \psi'_{k+1} \end{bmatrix} - \begin{bmatrix} R_k \\ 0 \end{bmatrix} y_k^C \right).$$

237 The top k rows of the parenthesized expression vanish by definition of y_k^C , and there
 238 remains

$$239 \quad \|r_k^C\| = (\beta_1 P_k^T e_1)_{k+1} = |\psi'_{k+1}|.$$

240 To derive recurrences for the residual norm for (NE), we can use the recurrences
 241 derived in Paige and Saunders (1975) for SYMMLQ and CG, which become

$$\begin{aligned}
 242 \quad \|A^T r_k^L\|^2 &= (\gamma_k \epsilon_k)^2 \zeta_k^2 + (\delta_k \eta_{k-1})^2 \zeta_{k-1}^2, \\
 243 \quad \|A^T r_k^C\| &= \alpha_1 \beta_1 s_1 \cdots s_{k-1} s_k / c_k.
 \end{aligned}$$

245 **2.5. Norm and condition number estimates.** Assuming orthonormality of
 246 V_k , (4) yields $V_k^T A^T AV_k = B_k^T B_k$, so that the Poincaré separation theorem ensures
 247 $\sigma_{\min}(A) \leq \sigma_{\min}(B_k) \leq \sigma_{\max}(B_k) \leq \sigma_{\max}(A)$ for all k , where σ_{\min} denotes the smallest
 248 nonzero singular value. Therefore we may use $\|B_k\|$ as an estimate of $\|A\|$ and $\text{cond}(B_k)$

Algorithm 2 LSLQ

```

1:  $\beta_1 u_1 = b, \alpha_1 v_1 = A^T u_1$  // begin Golub-Kahan process
2:  $\delta_1 = -1, \psi_1 = \beta_1$  // initialize variables
3:  $\tau_0 = \alpha_1 \beta_1, \zeta_0 = 0$ 
4:  $c_0 = 1, s_0 = 0$ 
5:  $\|A^T r_0^C\| = \alpha_1 \beta_1$ 
6:  $\bar{w}_1 = v_1, x_1^L = 0$ 
7: for  $k = 1, 2, \dots$  do
8:    $\beta_{k+1} u_{k+1} = A v_k - \alpha_k u_k$  // continue Golub-Kahan process
9:    $\alpha_{k+1} v_{k+1} = A^T u_{k+1} - \beta_{k+1} v_k$ 
10:   $\gamma_k = (\bar{\gamma}_k^2 + \beta_{k+1}^2)^{\frac{1}{2}}, c'_k = \bar{\gamma}_k / \gamma_k, s'_k = \bar{\beta}_{k+1} / \gamma_k$  // continue QR factorization
11:   $\delta_{k+1} = s'_k \alpha_{k+1}$ 
12:   $\bar{\gamma}_{k+1} = -c'_k \alpha_{k+1}$ 
13:   $\tau_k = -\tau_{k-1} \delta_k / \gamma_k$ 
14:   $\bar{\epsilon}_k = -\gamma_k c_{k-1}$  // continue LQ factorization
15:   $\eta_k = \gamma_k s_{k-1}$ 
16:   $\epsilon_k = (\bar{\epsilon}_k^2 + \delta_{k+1}^2)^{\frac{1}{2}}, c_k = \bar{\epsilon}_k / \epsilon_k, s_k = \delta_{k+1} / \epsilon_k$ 
17:   $\|r_{k-1}^L\| = ((\psi_{k-1} c'_k - \zeta_{k-1} \eta_k)^2 + (\psi_{k-1} s'_k)^2)^{\frac{1}{2}}$ 
18:   $\psi_k = \psi_{k-1} s'_k$ 
19:   $\|r_k^C\| = \psi_k$ 
20:   $\zeta_k = (\tau_k - \zeta_{k-1} \eta_k) / \epsilon_k$  // optional:  $\bar{\zeta}_k = \zeta_k / c_k$ 
21:   $\|A^T r_k^L\| = (\gamma_k^2 \epsilon_k^2 \zeta_k^2 + \delta_k^2 \eta_k^2 \zeta_{k-1}^2)^{\frac{1}{2}}$  // optional:  $\|A^T r_k^C\| = \|A^T r_{k-1}^C\| s_k c_{k-1} / c_k$ 
22:   $w_k = c_k \bar{w}_k + s_k v_{k+1}$ 
23:   $\bar{w}_{k+1} = s_k \bar{w}_k - c_k v_{k+1}$ 
24:   $x_{k+1}^L = x_k^L + \zeta_k w_k$  // optional:  $x_k^C = x_k^L + \bar{\zeta}_k \bar{w}_k$ 
25:   $\|x_{k+1}^L\|^2 = \|x_k^L\|^2 + \zeta_k^2$  // optional:  $\|x_{k+1}^C\|^2 = \|x_k^C\|^2 + \bar{\zeta}_k^2$ 
26: end for

```

249 as an estimate of $\text{cond}(A)$ in both the Euclidean and Frobenius norms. In particular,
250 $\|B_{k+1}\|_F^2 = \|B_k\|_F^2 + \alpha_k^2 + \beta_{k+1}^2$.

251 As in (Fong and Saunders, 2011, Section 3.4), our approximation of $\text{cond}(A)$ rests
252 on the QLP factorization

$$253 \quad P_k^T B_k Q_k^T = \begin{bmatrix} M_{k-1} & 0 \\ \eta_k e_{k-1}^T & \bar{\epsilon}_k \end{bmatrix}.$$

254 According to Stewart (1999), the absolute values of the diagonals of the bidiagonal
255 matrix above are tight approximations to the singular values of B_k . Thus we estimate

$$256 \quad \sigma_{\min}(B_k) \approx \min(\epsilon_1, \dots, \epsilon_{k-1}, |\bar{\epsilon}_k|), \quad \sigma_{\max}(B_k) \approx \max(\epsilon_1, \dots, \epsilon_{k-1}, |\bar{\epsilon}_k|),$$

257 and $\text{cond}(A) \approx \sigma_{\max}(B_k) / \sigma_{\min}(B_k)$, which turns out to be reasonably accurate in
258 practice. If b lies in a subspace spanned by only a few singular vectors of A , iterations
259 will terminate early and $\text{cond}(B_k)$ will be an improving estimate of $\text{cond}(A V_\ell)$.

260 **3. Complete algorithm.** The complete procedure is summarized as Algorithm 2.

261 As in (Fong and Saunders, 2011, Theorem 4.2), we can prove the following.

262 **THEOREM 2.** *LSLQ returns the MLS solution, i.e., it solves*

$$263 \quad \underset{x \in \mathbb{R}^n}{\text{minimize}} \|x\| \quad \text{subject to } x \in \underset{y}{\arg \min} \|A y - b\|.$$

264 **4. Error estimates.** In exact arithmetic, a least-squares solution x_\star is identified
 265 after at most $\ell \leq \min(m, n)$ iterations, so that $x_\star = x_{\ell+1}^L = \sum_{j=1}^{\ell} \zeta_j w_j$. Because
 266 $x_k^L = \sum_{j=1}^{k-1} \zeta_j w_j$, the error may be written as $e_k^L = x_{\ell+1}^L - x_k^L = \sum_{j=k}^{\ell} \zeta_j w_j$. By
 267 orthogonality, $\|e_k^L\|^2 = \sum_{j=k}^{\ell} \zeta_j^2$. A possible stopping condition is

$$269 \quad (27) \quad \|x_{k+1}^L - x_{k-d}^L\|^2 = \left(\sum_{j=k-d}^k \zeta_j^2 \right)^{\frac{1}{2}} \leq \varepsilon \|x_{k+1}^L\| \quad (k > d),$$

270 where $d \in \mathbb{N}$ is a delay and $0 < \varepsilon < 1$ is a tolerance. The left-hand side of (27) is a
 271 lower bound on the error $\|e_{k-d}^L\|$.

272 As we illustrate in section 6, (27) is not a robust stopping criterion because
 273 the lower bound may sometimes underestimate the actual error by several orders of
 274 magnitude. In the following sections, we develop a more robust estimate defined by
 275 an upper bound.

276 **4.1. Upper bound on the LSLQ error.** Estrin et al. (2016) develop an upper
 277 bound on the Euclidean error along SYMMLQ iterations for a symmetric positive
 278 semidefinite system. The bound leads to an upper bound on the error along CG
 279 iterations. We now translate those estimates to the present scenario and obtain upper
 280 bounds on the error along LSLQ and LSQR iterations for (LS) or (38). We begin with
 281 an upper bound on the LSLQ error. By orthogonality, $\|x_\star - x_k^L\|^2 = \|x_\star\|^2 - \|x_k^L\|^2$,
 282 and because $\|x_k^L\|^2$ can be computed, an upper bound on the error will follow from an
 283 upper bound on $\|x_\star\|^2$. Assume temporarily that $m \geq n$ and that A has full column
 284 rank, so that $A^T A$ is nonsingular. We may express

$$285 \quad \|x_\star\|^2 = b^T A (A^T A)^{-2} A^T b = b^T A f(A^T A) A^T b,$$

286 where $f(\xi) := \xi^{-2}$ is defined for all $\xi \in (0, \sigma_1^2]$, and where we define $f(A^T A) :=$
 287 $P f(\Sigma^T \Sigma) P^T$ with $A = Q \Sigma P^T$ the SVD of A . In other words, if p_i is the i -th column
 288 of P and σ_i is the i -th largest singular value of A ,

$$289 \quad f(A^T A) = \sum_{i=1}^n f(\sigma_i^2) p_i p_i^T.$$

290 We have from line 2 of Algorithm 1 and (6) that $A^T b = \bar{\beta}_1 v_1$ and therefore

$$291 \quad \|x_\star\|^2 = \bar{\beta}_1^2 \sum_{i=1}^n f(\sigma_i^2) \mu_i^2, \quad \mu_i := p_i^T v_1, \quad i = 1, \dots, n.$$

292 When A is rank-deficient, $A^T A$ is positive semidefinite and singular, but (NE)
 293 remains consistent. In addition, the MLS solution of (LS) lies in $\text{Range}(A^T)$. Let r
 294 be the smallest integer in $\{1, \dots, n\}$ such that $\sigma_{r+1} = \dots = \sigma_n = 0$ and $\sigma_r > 0$. Then
 295 $\text{rank}(A) = r = \dim \text{Range}(A^T)$ and the smallest nonzero eigenvalue of $A^T A$ is σ_r^2 . By
 296 the Rayleigh-Ritz theorem,

$$297 \quad \sigma_r^2 = \min \left\{ \|Av\|^2 \mid v \in \text{Range}(A^T), \|v\| = 1 \right\}.$$

298 Note that each $v_i \in \text{Range}(A^T)$ and that (4) implies $T_k = V_k^T A^T A V_k$ in exact arith-
 299 metic. Hence, for all $u \in \mathbb{R}^k$ with $\|u\| = 1$, we have $\|V_k u\| = 1$ and $u^T T_k u = \|A V_k u\|^2 \geq$
 300 $\sigma_r^2 > 0$, and each T_k is uniformly positive definite, despite the fact that $A^T A$ is singular.

301 Thus, in the rank-deficient case, $A^T A = \sum_{i=1}^r \sigma_i^2 p_i p_i^T$. The only difference with the
 302 full-rank case is that the sum occurs over all nonzero singular values of A . Therefore,
 303 we need only redefine

$$304 \quad (28) \quad f(\xi) := \begin{cases} \xi^{-2} & \text{if } x > 0 \\ 0 & \text{if } x = 0. \end{cases}$$

305 Because each x_k^L and each $x_k^C \in \text{Range}(A^T)$, the LSLQ and LSQR iterations occur
 306 in $\text{Range}(A^T)$ exactly as if they were applied to the r -by- r positive-definite system

$$307 \quad P_r^T A^T A P_r \bar{x} = P_r^T A^T b,$$

308 where $P_r = [p_1 \ \dots \ p_r]$ and $x_\star = P_r \bar{x}$. A consequence of the above discussion is
 309 that

$$310 \quad \|x_\star\|^2 = \bar{\beta}_1^2 \sum_{i=1}^r f(\sigma_i^2) \mu_i^2, \quad \mu_i := p_i^T v_1, \quad i = 1, \dots, n.$$

311 [Golub and Meurant \(1997\)](#) explain that the main insight is to view the previous
 312 sum as the Riemann-Stieltjes integral

$$313 \quad (29) \quad \sum_{i=1}^r f(\sigma_i^2) \mu_i^2 = \int_{\sigma_r}^{\sigma_1} f(\sigma^2) d\mu(\sigma),$$

314 where the piecewise constant Stieltjes measure μ is defined as

$$315 \quad \mu(\sigma) := \begin{cases} 0 & \text{if } \sigma < \sigma_r \\ \sum_{j=i}^r \mu_j^2 & \text{if } \sigma_i \leq \sigma < \sigma_{i+1} \\ \sum_{j=1}^r \mu_j^2 & \text{if } \sigma \geq \sigma_1. \end{cases}$$

316 Approximations to the integral via Gauss-related quadrature rules yield corresponding
 317 approximations to $\|x_\star\|^2$.

318 Our main result leading to an upper bound estimate follows from a Gauss-Radau
 319 approximation of (29) with a fixed quadrature node in $(0, \sigma_r^2)$. We begin with a
 320 paraphrase of ([Estrin et al., 2016](#), Theorem 2).

321 **PROPOSITION 3.** *Suppose $f : \mathbb{R} \rightarrow \mathbb{R}$ is such that $f^{(2j+1)}(\xi) < 0$ for all $\xi \in$
 322 (σ_r^2, σ_1^2) and all $j \geq 0$. Fix $\sigma_{est} \in (-\sigma_r, \sigma_r)$, $\sigma_{est} \neq 0$. Let T_k be the tridiagonal
 323 generated after k steps of [Algorithm 1](#) and $\varpi_k \in \mathbb{C}$ be chosen so that the smallest
 324 eigenvalue of*

$$325 \quad \tilde{T}_k := \begin{bmatrix} T_{k-1} & \bar{\beta}_k e_{k-1} \\ \bar{\beta}_k e_{k-1}^T & \alpha_k^2 + \varpi_k^2 \end{bmatrix}$$

326 *is precisely σ_{est}^2 . Then,*

$$327 \quad b^T A f(A^T A) A^T b \leq \bar{\beta}_1^2 e_1^T f(\tilde{T}_k) e_1.$$

328 In particular, [Proposition 3](#) applied to f defined in (28) provides an upper bound
 329 on $\|x_\star\|^2$.

330 Note that the Poincaré separation theorem ensures that the smallest eigenvalue of
 331 each T_{k-1} is at least σ_r^2 and that the Cauchy interlace theorem guarantees that the
 332 smallest eigenvalue of \tilde{T}_k is smaller than or equal to that of T_{k-1} . Thus it is possible
 333 to choose ϖ_k satisfying the requirements of [Proposition 3](#).

366 Note that \tilde{Y}_{2k} is a symmetric permutation of (32) and therefore shares the same eigen-
 367 values. If σ_{est} is an eigenvalue of \tilde{Y}_{2k} and $h^{(2k)} = [\theta_1 \ \dots \ \theta_{2k}]^T$ is a corresponding
 368 eigenvector, then $(\tilde{Y}_{2k} - \sigma_{\text{est}}I)h^{(2k)} = 0$; that is,

$$369 \begin{bmatrix} Y_{2k-2} - \sigma_{\text{est}}I & \delta_k e_{2k-2} & \\ \delta_k e_{2k-2}^T & -\sigma_{\text{est}} & \omega_k \\ & \omega_k & -\sigma_{\text{est}} \end{bmatrix} \begin{bmatrix} h_{2k-2}^{(2k)} \\ \theta_{2k-1} \\ \theta_{2k} \end{bmatrix} = 0.$$

370 Necessarily, $\theta_{2k-1} \neq 0$ because otherwise $h^{(2k)} = 0$ entirely. Thus we may fix $\theta_{2k-1} = 1$.
 371 The first block equation reads $(Y_{2k-2} - \sigma_{\text{est}}I)h_{2k-2}^{(2k)} = -\delta_k e_{2k-2}$. Let θ_{2k-2} be the last
 372 entry of $h_{2k-2}^{(2k)}$, which can be computed by updating the QR factors of Y_{2k-2} as in
 373 (Estrin et al., 2016).

374 In order to compute ω_k , note that the last two equations,

$$375 \begin{bmatrix} \delta_k & -\sigma_{\text{est}} & \omega_k \\ & \omega_k & -\sigma_{\text{est}} \end{bmatrix} \begin{bmatrix} \theta_{2k-2} \\ 1 \\ \theta_{2k} \end{bmatrix} = 0,$$

376 imply that $\omega_k = \sqrt{\sigma_{\text{est}}^2 - \delta_k \theta_{2k-2}}$.

377 With ω_k computed, we have $\tilde{R}_k^T \tilde{R}_k = \tilde{T}_k$. We are now interested in efficiently
 378 computing the upper bound

$$379 (33) \quad \|x_\star\|^2 \leq \bar{\beta}_1^2 e_1^T f(\tilde{R}_k^T \tilde{R}_k) e_1 = \bar{\beta}_1^2 e_1^T (\tilde{R}_k^T \tilde{R}_k)^{-2} e_1.$$

380 The LQ factorization $\tilde{R}_k = \tilde{M}_k \tilde{Q}_k$ provides the LQ factorization $\tilde{T}_k = \tilde{R}_k^T \tilde{M}_k \tilde{Q}_k$,
 381 which in turn yields

$$382 \|x_\star\|^2 \leq \left\| \bar{\beta}_1 \tilde{M}_k^{-1} \tilde{R}_k^{-T} e_1 \right\|^2 = \left\| \tilde{M}_k^{-1} \tilde{t}_k \right\|^2 = \left\| \tilde{z}_k \right\|^2,$$

383 where we define \tilde{t}_k and \tilde{z}_k from $\tilde{R}_k^T \tilde{t}_k = \bar{\beta}_1 e_1$ and $\tilde{M}_k \tilde{z}_k = \tilde{t}_k$ as in (Estrin et al., 2016).

384 We determine the LQ factorization $\tilde{R}_k = \tilde{M}_k \tilde{Q}_k$ from

$$385 \tilde{R}_k = \begin{bmatrix} R_{k-1} & \delta_k e_{k-1} \\ & \omega_k \end{bmatrix} = \begin{bmatrix} M_{k-1} & \\ \tilde{\eta}_k e_{k-1}^T & \tilde{\varepsilon}_k \end{bmatrix} \begin{bmatrix} Q_{k-1} & \\ & 1 \end{bmatrix}.$$

386 Thus $\tilde{Q}_k = Q_k$ and \tilde{M}_k differs from M_k in the $(k, k-1)$ -th and (k, k) -th entries only,
 387 which become

$$388 \tilde{\eta}_k = \omega_k s_{k-1}, \quad \tilde{\varepsilon}_k = -\omega_k c_{k-1}.$$

389 Recalling the definition of t_k in (19) and z_{k-1} in (20) we observe that

$$390 (34) \quad \tilde{t}_k = \begin{bmatrix} t_{k-1} \\ \tilde{\tau}_k \end{bmatrix} \quad \text{and} \quad \tilde{z}_k = \begin{bmatrix} z_{k-1} \\ \tilde{\zeta}_k \end{bmatrix},$$

391 where

$$392 (35) \quad \tilde{\tau}_k = -\tau_{k-1} \delta_k / \omega_k = \tau_k \gamma_k / \omega_k \quad \text{and} \quad \tilde{\zeta}_k = (\tilde{\tau}_k - \tilde{\eta}_k \zeta_{k-1}) / \tilde{\varepsilon}_k.$$

393 From (24) and orthogonality of W_k we now have

$$394 (36) \quad \|x_\star - x_k^L\|^2 = \|x_\star\|^2 - \|x_k^L\|^2 \leq \|z_{k-1}\|^2 + \tilde{\zeta}_k^2 - \|z_{k-1}\|^2 = \tilde{\zeta}_k^2.$$

395 **4.2. Upper bound on the LSQR error.** Obtaining an upper bound on the
 396 LSQR error is of interest for two reasons. First, LSLQ may transfer to the LSQR
 397 point at any iteration using a simple vector operation—see (22). Second, LSQR always
 398 produces a smaller error, as formalized by Proposition 1.

399 Based on Proposition 1, we wish to use the upper bound (36) and the transition
 400 (22) to the LSQR point to terminate LSLQ early and obtain an iterate with an error
 401 below a prescribed level. Evidently the same upper bound (36) could be used, but
 402 Estrin et al. (2016) provide the improved bound

$$403 \quad (37) \quad \|x_\star - x_k^C\|^2 \leq \tilde{\zeta}_k^2 - \bar{\zeta}_k^2,$$

404 where $\bar{\zeta}_k$ is defined in (20) and $\tilde{\zeta}_k$ is in (35).

405 **5. Regularization.** LSLQ may be adapted to solve the regularized least-squares
 406 problem

$$407 \quad (38) \quad \underset{x \in \mathbb{R}^n}{\text{minimize}} \quad \frac{1}{2} \left\| \begin{bmatrix} A \\ \lambda I \end{bmatrix} x - \begin{bmatrix} b \\ 0 \end{bmatrix} \right\|^2,$$

408 where $\lambda \geq 0$ is a given regularization parameter. The optimality conditions (NE)
 409 become

$$410 \quad (39) \quad (A^T A + \lambda^2 I)x = A^T b.$$

411 If we run Algorithm 1 on A only, we will produce the factorization

$$412 \quad (40) \quad \begin{bmatrix} A \\ \lambda I \end{bmatrix} V_k = \begin{bmatrix} U_{k+1} & \\ & V_k \end{bmatrix} \begin{bmatrix} B_k \\ \lambda I \end{bmatrix},$$

413 which we can compare to the factorization achieved when running Algorithm 1 on the
 414 entire regularized system,

$$415 \quad (41) \quad \begin{bmatrix} A \\ \lambda I \end{bmatrix} V_k = \hat{U}_{k+1} \hat{B}_k = \hat{U}_{k+1} \begin{bmatrix} \hat{\alpha}_1 & & & \\ \hat{\beta}_2 & \ddots & & \\ & \ddots & \hat{\alpha}_k & \\ & & & \hat{\beta}_{k+1} \end{bmatrix}.$$

416 Note that V_k will remain unchanged, as can be seen from the equivalence between the
 417 Golub-Kahan process and the Lanczos process on the normal equations (Saunders,
 418 1995). Given \hat{B}_k , we could run the non-regularized LSLQ algorithm (using $\hat{\alpha}$ and $\hat{\beta}$
 419 instead of α and β) to obtain all of the desired iterates and estimates. The idea is
 420 therefore to compute B_k via Golub-Kahan on (A, b) , cheaply compute each $\hat{\alpha}_k$ and
 421 $\hat{\beta}_k$ and use them in place of α_k and β_k in the rest of the algorithm. For $k = 3$, the

422 factorization proceeds according to

$$\begin{aligned}
 & \begin{bmatrix} \alpha_1 & & & & & \\ \beta_2 & \alpha_2 & & & & \\ & \beta_3 & \alpha_3 & & & \\ & & \beta_4 & & & \\ \lambda & & & & & \\ & \lambda & & & & \\ & & & \lambda & & \end{bmatrix} \rightarrow \begin{bmatrix} \alpha_1 & & & & & \\ \hat{\beta}_2 & \hat{\alpha}_2 & & & & \\ & \beta_3 & \alpha_3 & & & \\ & & \hat{\lambda}_2 & & & \\ & & \lambda & & & \\ & & & \lambda & & \end{bmatrix} \rightarrow \begin{bmatrix} \alpha_1 & & & & & \\ \hat{\beta}_2 & \hat{\alpha}_2 & & & & \\ & \beta_3 & \alpha_3 & & & \\ & & & \lambda_2 & & \\ & & & & \lambda & \end{bmatrix} \\
 423 \quad (42) \quad & \rightarrow \begin{bmatrix} \alpha_1 & & & & & \\ \hat{\beta}_2 & \hat{\alpha}_2 & & & & \\ & \hat{\beta}_3 & \hat{\alpha}_3 & & & \\ & & \beta_4 & & & \\ & & & \hat{\lambda}_3 & & \\ & & & \lambda & & \end{bmatrix} \rightarrow \begin{bmatrix} \alpha_1 & & & & & \\ \hat{\beta}_2 & \hat{\alpha}_2 & & & & \\ & \hat{\beta}_3 & \hat{\alpha}_3 & & & \\ & & \beta_4 & & & \\ & & & \lambda_3 & & \end{bmatrix}
 \end{aligned}$$

424 We use β_{k+1} to zero out λ_k , which transforms α_{k+1} into $\hat{\alpha}_{k+1}$ and introduces a nonzero
 425 $\hat{\lambda}_{k+1}$ above λ in the next column. We then use a second reflection to zero out $\hat{\lambda}_{k+1}$
 426 using λ , which produces λ_{k+1} . With $\lambda_1 = \lambda$, the recurrences for $k \geq 2$ are

$$\begin{aligned}
 & \hat{\beta}_{k+1} = (\beta_{k+1}^2 + \lambda_k^2)^{\frac{1}{2}}, \\
 & c_k^L = \beta_{k+1} / \hat{\beta}_{k+1}, \\
 & s_k^L = \lambda_k / \hat{\beta}_{k+1}, \\
 427 \quad (43) \quad & \hat{\alpha}_{k+1} = c_k^L \alpha_{k+1}, \\
 & \hat{\lambda}_{k+1} = s_k^L \alpha_{k+1}, \\
 & \lambda_{k+1} = (\lambda^2 + \hat{\lambda}_{k+1}^2)^{\frac{1}{2}}.
 \end{aligned}$$

428 With $\lambda > 0$, the operator of (38) has full column rank, i.e., $r = n$, and satisfies
 429 $\sigma_n \geq \lambda$. [Theorem 4](#) then states that we should select $\sigma_{\text{est}} \in (0, \lambda)$.

430 **6. Numerical experiments.** In the experiments reported here, the exact solu-
 431 tion of (LS) was computed as the MLS solution using a complete orthogonal decom-
 432 position of A via the `Factorize` package ([Davis, 2013](#)). The horizontal axis in plots
 433 represents iterations, each involving a product with A and a product with A^T . LSLQ
 434 is implemented in the Julia language ([julialang.org](#)) and is available as part of the
 435 `Krylov.jl` suite of iterative methods ([Orban, 2017](#)). [Subsection 6.1](#) and [subsection 6.2](#)
 436 document our results on problems from the animal breeding test set and on the seismic
 437 inversion problem described in [section 1](#), respectively. Although all test problems
 438 are over-determined, the solvers apply to systems of any shape. We have observed
 439 qualitatively similar results for square and underdetermined systems.

440 **6.1. Problems from the animal breeding test set.** In this section, we use
 441 test problems from the animal breeding collection of [Hegland \(1990, 1993\)](#). These
 442 over-determined problems have rank-deficiency 1, come in two flavors and sizes, and
 443 have accompanying right-hand sides. In the first flavor, a single parameter is fitted
 444 per animal, while in the second flavor, two parameters are fitted per animal and A
 445 has twice as many rows and columns. The nonzero columns of A are scaled to have
 446 unit Euclidean norm.

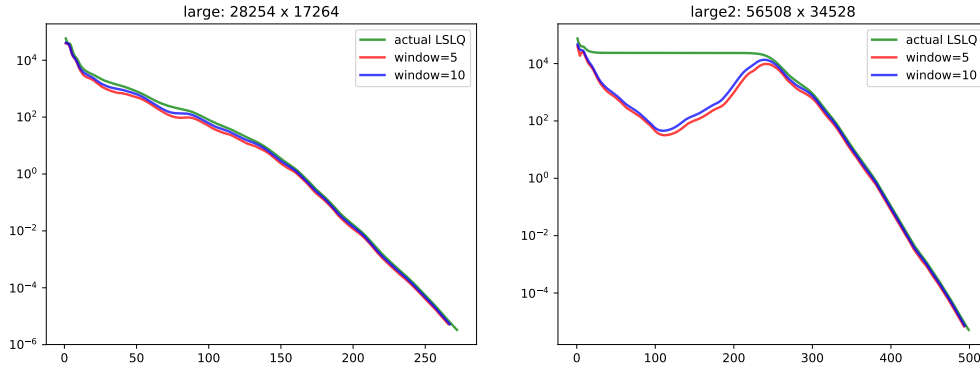


FIG. 2. Error along the LSLQ iterations on problems *large* and *large2* from the animal breeding set. The red and blue curves show the lower bounds with $d = 5$ and $d = 10$.

447 We found that generating the problems from the original archive requires a small
 448 amount of corrections to the programs and several compilation steps. Because we feel
 449 that the problems from this set are generally useful as least-squares test problems,
 450 we have created an archive containing the problems as well as the MLS solutions
 451 corresponding to the scaled problems in Rutherford-Boeing format (Duff, Grimes,
 452 and Lewis, 1997). Our repository can be accessed at github.com/optimizers/animal
 453 (Orban, 2016).

454 We begin with an illustration of the non-robust lower bound (27) based on a
 455 delay d . Figure 2 plots the actual LSLQ error along with the lower bound with delay
 456 (window size) $d = 5$ and 10 iterations for problems *large* and *large2* (larger versions
 457 of the problems used in Figure 1). The behavior seen is typical. As in the left-hand
 458 plot, the lower bound tends to follow the exact error curve tightly when the latter is
 459 strictly decreasing. But as the right-hand plot shows, it tends to underestimate the
 460 actual error by several orders of magnitude when the latter plateaus, and requires a
 461 fair number of iterations to recover, rendering the stopping test unreliable by itself. In
 462 both plots, the stopping test used is (27) with $\varepsilon = 10^{-10}$. The curves for $d = 5$ and 10
 463 are almost the same.

464 Figure 3 illustrates the behavior of our upper bound (36) on problems *large* and
 465 *large2* with regularization: a typical scenario for rank-deficient problems whose smallest
 466 nonzero singular value is unknown. For a given value $\lambda \neq 0$, the smallest singular
 467 value of the regularized A is $\sigma_n = |\lambda|$. Estrin et al. (2016) show numerically that the
 468 upper bound is tighter when $|\sigma_{\text{est}}|$ is closer to $|\sigma_n|$, but they do not consider the effect
 469 of regularization. To simplify the discussion, we consider only positive values of λ . For
 470 each value of $\lambda > 0$, we set $\sigma_{\text{est}} := (1 - 10^{-10})\lambda$ and measure the error with respect
 471 to the solution of the regularized problem.

472 We observe from Figure 3 that increasing λ (and hence σ_{est}) substantially improves
 473 the quality of the upper bound. The reason may be that \tilde{T}_k is moved further away from
 474 singularity. In the case of *large2* with $\lambda = 10^{-2}$, the upper bound is exceptionally tight
 475 after about 100 iterations. As λ decreases, the upper bound deteriorates, although it
 476 remains a potentially useful bound as long as $\lambda \neq 0$.

477 In Figure 4, we compute the bound (37) on the error along the LSQR iterates or,
 478 equivalently, along the LSQR points obtained by transitioning from a corresponding
 479 LSLQ point. As with LSLQ, the quality of the LSQR upper bound deteriorates
 480 when A , or its regularization, approaches rank-deficiency. The LSQR bound appears

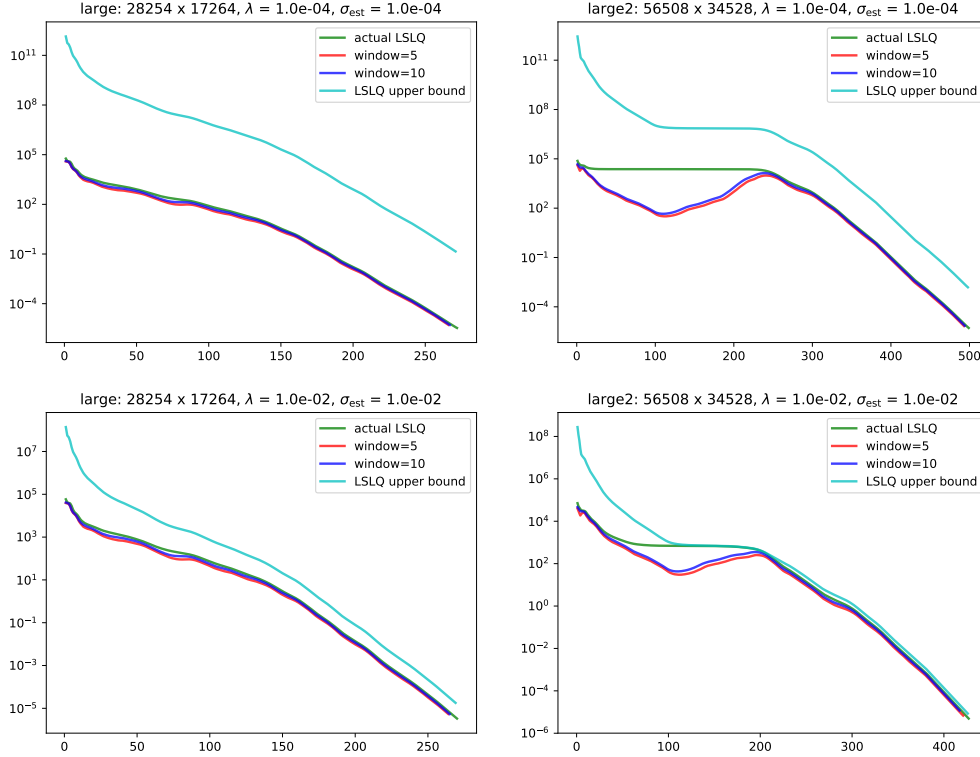


FIG. 3. Error along the LSLQ iterations on problems *large* and *large2* with regularization. The red and blue curves show the lower bounds with $d = 5$ and $d = 10$. The cyan curve shows the upper bounds for $\lambda = 10^{-4}$ (top) and $\lambda = 10^{-2}$ (bottom).

481 somewhat looser than the LSLQ bound, although [Estrin et al. \(2016\)](#) note that it
 482 could be tightened by incorporating an additional term along a moving window to the
 483 right-hand side of (37).

484 The next experiment illustrates the upper bounds for rank-deficient problems when
 485 we have knowledge of σ_r . A sparse SVD reveals that the smallest nonzero singular
 486 value after scaling is approximately $\sigma_r = \sigma_{n-1} \approx 0.0498733$ for problem *small* and
 487 $\sigma_r = \sigma_{n-1} \approx 0.00499044$ for *small2*. In each case, we set $\sigma_{\text{est}} = (1 - 10^{-10}) \sigma_{n-1}$. In
 488 practice, one may need to underestimate further in order to account for inaccurate σ_r .

489 As the error bounds in [Figure 5](#) are quite tight, it seems important to supply an
 490 estimate of σ_r in rank-deficient problems if such knowledge is available. In [Figure 5](#),
 491 LSLQ stops as soon as the upper bound on the LSQR error falls below $10^{-10} \|x_k^C\|$.

492 **6.2. The seismic inverse problem.** The least-squares problem arising from
 493 the PDE-constrained optimization problem described in [section 1](#) has the form

$$494 \quad (44) \quad \underset{x \in \mathbb{R}^n}{\text{minimize}} \quad \frac{1}{2} \left\| \begin{bmatrix} \rho A \\ P \end{bmatrix} x - \begin{bmatrix} \rho q \\ d \end{bmatrix} \right\|^2,$$

495 where $\rho = 0.1$ is fixed, A is a square 5-point stencil discretization of a Helmholtz
 496 operator, P is a sampling operator (some rows of the identity), and q and d are fixed
 497 vectors. We experimented with a case in which $n = 83,600$ and P has 248 rows. The
 498 columns of the operator were not scaled as in the previous section, as that reduced

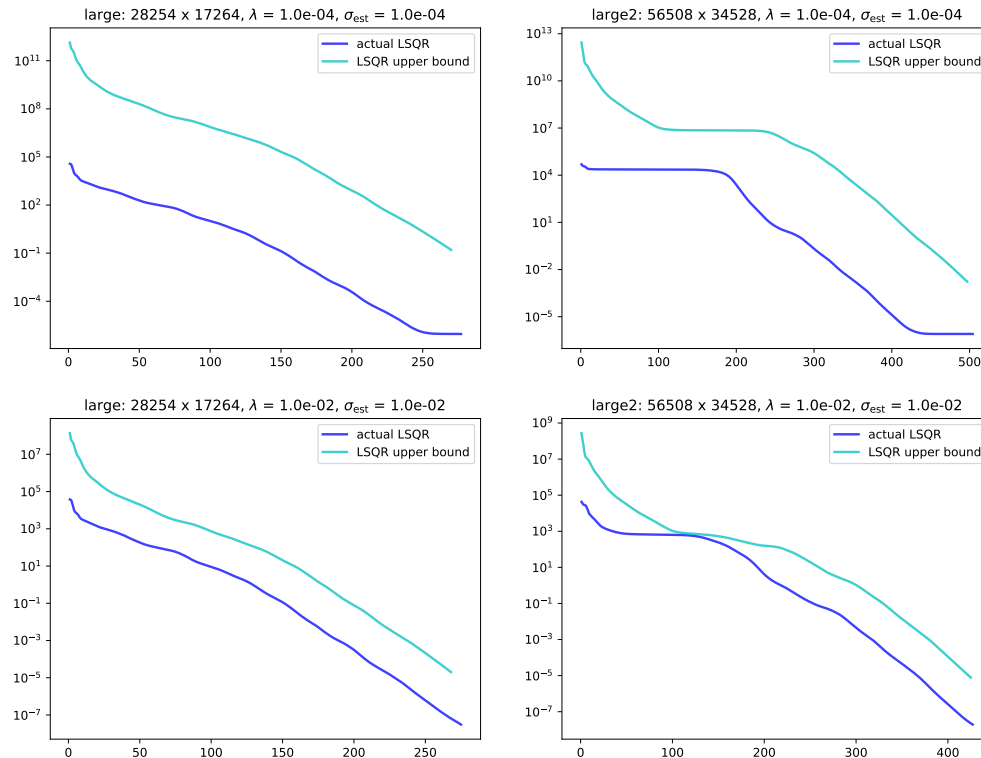


FIG. 4. Error along the LSQR iterations on problems `large` and `large2` with regularization. The cyan curve shows the upper bounds for $\sigma_{est} = 10^{-4}$ (top) and $\sigma_{est} = 10^{-2}$ (bottom).

499 the performance of LSLQ. A complete orthogonal decomposition, used to compute the
500 exact solution, reveals that the operator of (44) has full rank but its smallest nonzero
501 singular value is $O(10^{-6})$. A partial sparse SVD suggests that there are several small
502 singular values. To obtain upper error bounds, it was necessary to set $\sigma_{est} = 10^{-7}$ to
503 avoid domain errors in computing the square root in the expression for ω_k preceding
504 (33). The left plots of Figure 6 illustrate the upper and lower bounds on the error
505 and the large number of iterations needed to decrease the error by a factor of 10^{10} .
506 The bounds on the LSLQ and LSQR errors nonetheless track the exact errors quite
507 accurately, with the upper bound on the LSQR error overestimating by one or two
508 orders of magnitude. Though the factor 10^{10} is far too demanding in practice, it
509 illustrates that many iterations are likely when there are many tiny singular values.
510 The situation is similar when the problem is regularized and the error is measured with
511 respect to the exact solution of the original, unregularized, problem. The right plots of
512 Figure 6 show the bounds in the presence of modest regularization λ when the error is
513 computed with respect to the exact solution of the regularized problem. Dramatically
514 fewer iterations are needed to achieve a corresponding decrease in the error. Note
515 the remarkable tightness of the LSLQ and LSQR bounds, with the LSQR upper
516 bound consistently overestimating by about one order of magnitude. The improved
517 performance on the regularized problem suggests that a regularized optimization
518 approach, such as that of Arreckx and Orban (2016), could be appropriate.

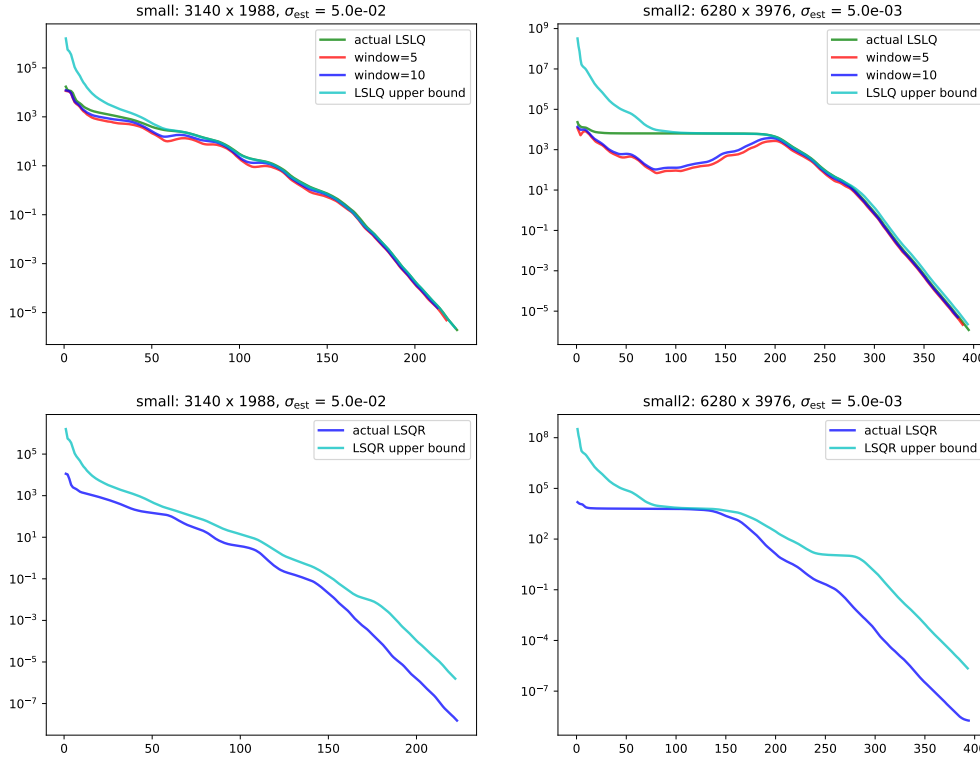


FIG. 5. Error along the LSLQ and LSQR iterations on problems *small* and *small2* without regularization. Both problems have rank-deficiency 1.

519 **7. Discussion.** LSLQ is an iterative method for the least-squares and least-
 520 norm problems (LS) and (LN) with the attractive property that it ensures monotonic
 521 reduction in the Euclidean error $\|x - x_k\|_2$. In deriving it we have completed the triad
 522 of solvers LSQR, LSMR, LSLQ for problem (LS) based on the Golub and Kahan (1965)
 523 process. They are mathematically equivalent to the symmetric solvers CG, MINRES,
 524 SYMMLQ on (NE) but are numerically more reliable when A is ill-conditioned.

525 Although the Euclidean error for LSQR is provably better at each iterate, it is
 526 possible to develop cheaply computable lower and upper bounds on the error for LSLQ.
 527 The intimate relationship between the methods, analogous to that between CG and
 528 SYMMLQ (Estrin et al., 2016), provides a corresponding upper bound on the LSQR
 529 error at each iteration. Such an upper bound was not previously available. It may be
 530 used in a stopping criterion to terminate LSLQ and transfer to the LSQR point.

531 Strakoš and Tichý (2002) justify the adequacy of A -norm error estimates for CG
 532 by way of a finite-precision arithmetic analysis. The upper bounds described in the
 533 present paper assume exact arithmetic and orthogonality of the Golub-Kahan bases. In
 534 the numerical experiments, our aim has been to observe if the theoretical upper bounds
 535 remain upper bounds in practice. They appear to do so up to the point of convergence,
 536 as they do for CG and SYMMLQ. We conclude that a future finite-precision analysis
 537 is justified.

538 Fong and Saunders (2012, Table 5.1) summarize the monotonicity of various
 539 quantities related to the LSQR and LSMR iterations. Table 1 is similar but focuses
 540 on LSQR and LSLQ.

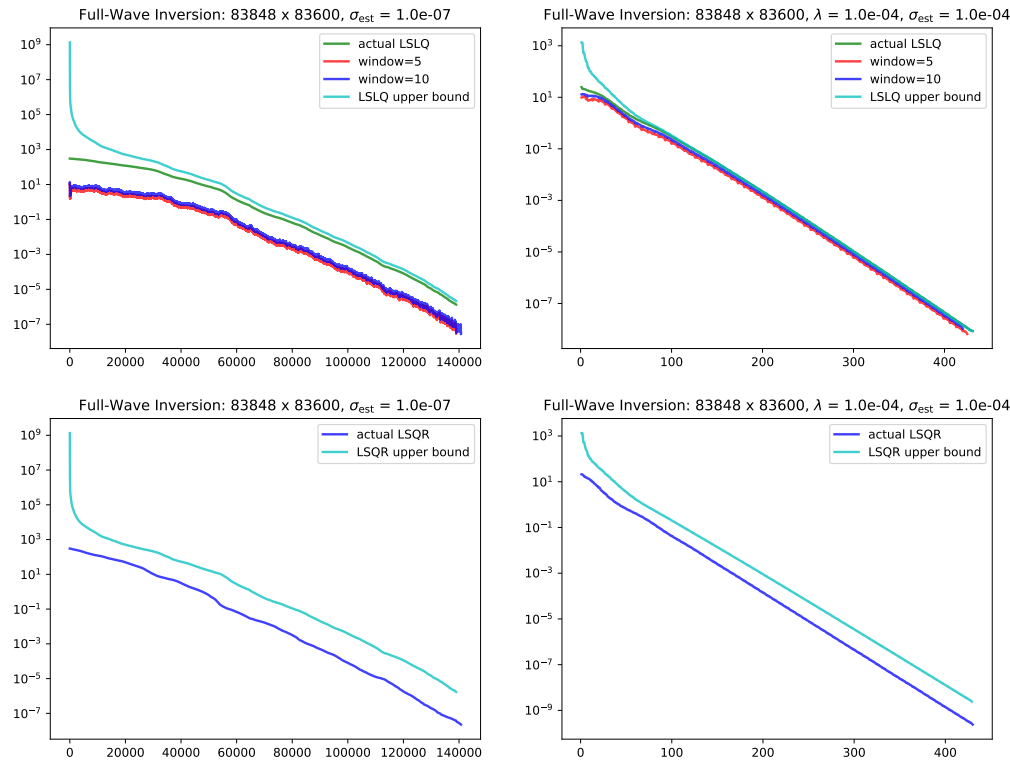


FIG. 6. Error along the LSLQ and LSQR iterations on the seismic inverse problem without regularization (left) and with regularization (right).

TABLE 1
Comparison of LSQR and LSLQ properties on a linear least-square problems $\min \|Ax - b\|$.

	LSQR	LSLQ
$\ x_k\ $	\nearrow (F, 2011, Theorem 3.3.1)	\nearrow (PS, 1975), \leq LSQR (Proposition 1)
$\ x_\star - x_k\ $	\searrow (F, 2011, Theorem 3.3.2)	\searrow (PS, 1975), \geq LSQR (Proposition 1)
$\ r_\star - r_k\ $	\searrow (F, 2011, Theorem 3.3.3)	not-monotonic
$\ r_k\ $	\searrow	not-monotonic
$\ A^T r_k\ $	not-monotonic	not-monotonic
x_k converges to MLS on column-rank-deficient problems		
	\nearrow monotonically increasing	\searrow monotonically decreasing
	F (Fong, 2011), PS (Paige and Saunders, 1975)	

541 Saunders, Simon, and Yip (1988) develop the USYMLQ method based on an
 542 orthogonal tridiagonalization process that applies to square systems. USYMLQ only
 543 applies to consistent systems and, analogous to SYMMLQ, reduces the Euclidean
 544 error monotonically. Because the orthogonal tridiagonalization process reduces to the
 545 Lanczos (1950) process in the symmetric case, USYMLQ applied to (NE) must be
 546 equivalent to SYMMLQ applied to (NE), and therefore to LSLQ applied to (LS), in
 547 exact arithmetic. However, applying USYMLQ to (NE) would perform redundant
 548 work and require two products with $A^T A$ per iteration.

549 **7.1. A generalization.** LSLQ may be generalized to the solution of symmetric
550 quasi-definite systems (Vanderbei, 1995) of the form

$$551 \quad (45) \quad \begin{bmatrix} M & A \\ A^T & -N \end{bmatrix} \begin{bmatrix} r \\ x \end{bmatrix} = \begin{bmatrix} b \\ 0 \end{bmatrix},$$

552 where $M = M^T$ and $N = N^T$ are positive definite. Indeed (45) represents the
553 optimality conditions of

$$554 \quad (46) \quad \underset{x \in \mathbb{R}^n}{\text{minimize}} \quad \frac{1}{2} \left\| \begin{bmatrix} A \\ I \end{bmatrix} x - \begin{bmatrix} b \\ 0 \end{bmatrix} \right\|_E^2,$$

555 where $E = \text{blkdiag}(M^{-1}, N)$. Under the assumption that solves with M and N can
556 be performed cheaply, which is the case in certain optimization schemes and fluid
557 flow simulations (Orban and Arioli, 2017), it suffices to replace the Golub-Kahan
558 process (Algorithm 1) with its preconditioned variant, stated as (Orban and Arioli,
559 2017, Algorithm 4.2), and to set the regularization parameter $\lambda = 1$.

560 Note that (45) also represents the optimality conditions of the *least-norm* problem

$$561 \quad (\text{LN2}) \quad \underset{x \in \mathbb{R}^n, s \in \mathbb{R}^m}{\text{minimize}} \quad \frac{1}{2} (\|r\|_M^2 + \|x\|_N^2) \quad \text{subject to } Mr + Ax = b.$$

562 We may construct a companion method to LSLQ that solves (LN2) by implicitly
563 applying SYMMLQ to the normal equations of the second kind, which in this case are

$$564 \quad (\text{NE2}) \quad (AN^{-1}A^T + M)r = b, \quad Nx = A^T r.$$

565 This variant, let us call it LNLQ, is to LSLQ as the method of Craig (1955) is to
566 LSQR. Following the same reasoning as Saunders (1995) and Orban and Arioli (2017),
567 it appears possible to show that applying SYMMLQ to (45) with preconditioner
568 $\text{blkdiag}(M, N)$ is equivalent to applying LSLQ to (46) and LNLQ to (LN2) simulta-
569 neously. If so, SYMMLQ applied to (45) would perform twice the work by solving the
570 two equivalent problems (NE) and (NE2) simultaneously, making a solver for (LN2)
571 worthwhile. An implementation of LNLQ is the subject of ongoing work.

572 **Acknowledgements.** We are grateful to Tristan van Leeuwen for supplying code
573 that allowed us to generate instances of the seismic inverse problem. We are also
574 deeply grateful to the referees for their insightful recommendations.

575 **References.**

- 576 S. Arreckx and D. Orban. A regularized factorization-free method for equality-
577 constrained optimization. Cahier du GERAD G-2016-65, GERAD, Montréal, QC,
578 Canada, 2016.
- 579 A. R. Conn, N. I. M. Gould, and Ph. L. Toint. *Trust-Region Methods*, volume 1
580 of *MPS/SIAM Series on Optimization*. SIAM, Philadelphia, USA, 2000. DOI:
581 [10.1137/1.9780898719857](https://doi.org/10.1137/1.9780898719857).
- 582 J. E. Craig. The N-step iteration procedures. *Journal of Mathematics and Physics*, 34
583 (1):64–73, 1955.
- 584 T. A. Davis. Algorithm 930: FACTORIZE: An object-oriented linear system
585 solver for matlab. *ACM Trans. Math. Softw.*, 39(4):28:1–28:18, July 2013. DOI:
586 [10.1145/2491491.2491498](https://doi.org/10.1145/2491491.2491498).
- 587 I. S. Duff, R. G. Grimes, and J. G. Lewis. The Rutherford-Boeing sparse matrix
588 collection. Technical Report RAL-TR-97-031, Rutherford Appleton Laboratory,
589 Chilton, OX, UK, 1997.

- 590 R. Estrin, D. Orban, and M. A. Saunders. Euclidean-norm error bounds for CG via
591 SYMMLQ. Cahier du GERAD G-2016-70, GERAD, Montréal, QC, Canada, 2016.
- 592 D. C.-L. Fong. Minimum-residual methods for sparse least-squares using golub-kahan
593 bidiagonalization, December 2011.
- 594 D. C.-L. Fong and M. A. Saunders. LSMR: An iterative algorithm for sparse
595 least-squares problems. *SIAM J. Sci. Comput.*, 33(5):2950–2971, 2011. DOI:
596 [10.1137/10079687X](https://doi.org/10.1137/10079687X).
- 597 D. C.-L. Fong and M. A. Saunders. CG versus MINRES: An empirical comparison.
598 *SQU Journal for Science*, 17(1):44–62, 2012.
- 599 G. H. Golub and W. Kahan. Calculating the singular values and pseudo-inverse of a
600 matrix. *SIAM J. Numer. Anal.*, 2(2):205–224, 1965. DOI: [10.1137/0702016](https://doi.org/10.1137/0702016).
- 601 G. H. Golub and G. Meurant. Matrices, moments and quadrature II; how to compute
602 the norm of the error in iterative methods. *BIT Num. Math.*, 37(3):687–705, 1997.
603 DOI: [10.1007/BF02510247](https://doi.org/10.1007/BF02510247).
- 604 M. Hegland. *On the computation of breeding values*, pages 232–242. Springer Berlin
605 Heidelberg, Berlin, Heidelberg, 1990. ISBN 978-3-540-46597-3. DOI: [10.1007/3-540-
606 53065-7_103](https://doi.org/10.1007/3-540-53065-7_103).
- 607 M. Hegland. Description and use of animal breeding data for large least squares
608 problems. Technical Report TR/PA/93/50, CERFACS, Toulouse, France, 1993.
- 609 M. R. Hestenes and E. Stiefel. Methods of conjugate gradients for solving linear
610 systems. *J. Res. N.B.S.*, 49(6):409–436, 1952.
- 611 C. Lanczos. An iteration method for the solution of the eigenvalue problem of linear
612 differential and integral operators. *J. Res. N.B.S. B*, 45:225–280, 1950.
- 613 G. Meurant. Estimates of the l2 norm of the error in the conjugate gradient algorithm.
614 *Numerical Algorithms*, 40(2):157–169, 2005. DOI: [10.1007/s11075-005-1528-0](https://doi.org/10.1007/s11075-005-1528-0).
- 615 D. Orban. optimizers/animal: Initial release, December 2016. URL [https://github.
616 com/optimizers/animal](https://github.com/optimizers/animal).
- 617 D. Orban. Krylov.jl suite of iterative methods, July 2017. URL [https://github.com/
618 JuliaSmoothOptimizers/Krylov.jl](https://github.com/JuliaSmoothOptimizers/Krylov.jl).
- 619 D. Orban and M. Arioli. *Iterative Methods for Symmetric Quasi-Definite Linear
620 Systems*. Number 03 in Spotlights. SIAM, Philadelphia, PA, 2017. ISBN 978-1-
621 611974-72-0.
- 622 C. C. Paige and M. A. Saunders. Solution of sparse indefinite systems of linear
623 equations. *SIAM J. Numer. Anal.*, 12(4):617–629, 1975. DOI: [10.1137/0712047](https://doi.org/10.1137/0712047).
- 624 C. C. Paige and M. A. Saunders. LSQR: An algorithm for sparse linear equations
625 and sparse least squares. *ACM Trans. Math. Softw.*, 8(1):43–71, 1982a. DOI:
626 [10.1145/355984.355989](https://doi.org/10.1145/355984.355989).
- 627 C. C. Paige and M. A. Saunders. Algorithm 583; LSQR: Sparse linear equations
628 and least-squares problems. *ACM Trans. Math. Softw.*, 8(2):195–209, 1982b. DOI:
629 [10.1145/355993.356000](https://doi.org/10.1145/355993.356000).
- 630 M. A. Saunders. Solution of sparse rectangular systems using LSQR and CRAIG. *BIT
631 Num. Math.*, 35:588–604, 1995. DOI: [10.1007/BF01739829](https://doi.org/10.1007/BF01739829).
- 632 M. A. Saunders, H. D. Simon, and E. L. Yip. Two conjugate-gradient-type methods
633 for unsymmetric linear equations. *SIAM J. Numer. Anal.*, 25(4):927–940, 1988.
634 DOI: [10.1137/0725052](https://doi.org/10.1137/0725052).
- 635 G. W. Stewart. The QLP approximation to the singular value decomposition. *SIAM
636 J. Sci. Comput.*, 20(4):1336–1348, 1999. DOI: [10.1137/S1064827597319519](https://doi.org/10.1137/S1064827597319519).
- 637 Z. Strakoš and P. Tichý. On error estimation in the conjugate gradient method and
638 why it works in finite precision. *Elec. Trans. Numer. Anal.*, 13, 2002.
- 639 T. Van Leeuwen and F. J. Herrmann. A penalty method for PDE-constrained op-

- 640 timization. Technical Report TR-EOAS-2013-6, University of British Columbia,
641 2013.
- 642 R. J. Vanderbei. Symmetric quasi-definite matrices. *SIAM J. Optim.*, 5(1):100–113,
643 1995. DOI: [10.1137/0805005](https://doi.org/10.1137/0805005).